https://jos.unsoed.ac.id/index.php/exj/

E-ISSN : xxxxxxxxx
P-ISSN : xxxxxxxxx

EarthXplorer Journal

Vol 01 No 01 2025

RESEARCH ARTICLE

PETROLOGICAL CHARACTERISTICS AND COOLING DYNAMICS OF MOUNT PARANG AND MOUNT BONGKOK INTRUSION, PURWAKARTA, WEST JAVA

Bayu Pamungkas, Rio Priandri Nugroho[1,*]

[1] Geological Engineering, Universitas Pertamina

* *Corresponding author* : rio.priandri@universitaspertamina.ac.id

Received: July 3, 2025; Accepted: July 30, 2025.

Abstract

Mount Parang and Mount Bongkok in Purwakarta, West Java, are prominent and well-exposed intrusive bodies that offer valuable insights into subvolcanic magmatic processes in the region. Despite their geological significance, detailed investigations into their magmatic evolution and crystallization histories remain scarce. This study aims to characterize the petrology and unravel the crystallization dynamics of these intrusive complexes through petrographic analysis and Crystal Size Distribution (CSD) modeling of plagioclase phenocrysts. Field and microscopic observations reveal that both bodies are composed predominantly of andesite, containing phenocrysts of plagioclase, hornblende, and pyroxene, with minor variations in bulk composition. Magma mixing and assimilation are interpreted based on the presence of mafic rock fragments, oscillatory zoning, and sieve textures. CSD analysis constrains the minimum crystallization duration of the Mount Parang magma to at least 11.74 years, while Mount Bongkok's magma is estimated to have crystallized over at least 10.93 years. These durations reflect only the phenocryst growth phase, as groundmass cooling times were not included. The results contribute to a better understanding of the timescales and processes governing sub-volcanic intrusion and magma evolution of other intrusive complex with similar ages in the surrounding area.

Keywords: Mount Parang, Mount Bongkok, Petrography, Crystal Size Distribution (CSD), crystallization duration.

1. Introduction

The subduction of the Eurasian and Indo-Australian plates has resulted in the formation of a magmatic arc extending along the islands of Sumatra, Java, and Banda, characterized by a chain of volcanoes and the distribution of intrusive igneous rocks (Katili, 1975). By studying the characteristics of exposed intrusive igneous rocks, it is possible to interpret the petrogenesis and magmatic processes that occurred in the geological past. This, in turn, provides an analogue for understanding similar processes that are ongoing in the present day.

In the Purwakarta region, several intrusive igneous bodies are well-exposed, particularly at Mount Parang and Mount Bongkok (Sudjatmiko, 1972). Therefore, this area represents an ideal setting for investigating petrogenetic characteristics within a complex of intrusive bodies. Currently, petrological research in the area is limited to petrogenetic characterization (Arfiansyah and Helmi, 2018) and alteration (Lestianingrum and Wijaya, 2020) without temporal constraint. This study presents the results of petrographic analysis and crystal size distribution (CSD) of rock samples collected from Mount Parang and Mount Bongkok, aiming to unravel the magmatic processes involved, including the timescales of crystallization within these spatially associated intrusive bodies during their emplacement. Application of CSD on intrusive bodies has been reported to explain their magma dynamics and temporal constraints (e.g. Ashok et al., 2022; Magee et al., 2010; Patwardhan and Marsh, 2011; Sobolev et al., 2023). In addition, the result of this study, in term of magma dynamics of sub-volcanic intrusion, may give hints in understanding of later stage hydrothermal alterations and mineralization that occur in the area.

2. Geological Setting

The tectonic evolution of West Java (Figure 1) is described in detail by Clements and Hall (2007). During the Early Miocene, intense volcanic activity

began to occur in the southern part of Java, significantly influencing depositional processes in West Java. Rapid volcanic deposition led to a transition in the sedimentary system within the Bogor Basin, resulting in the development of gravity-driven deposits. By the Middle Miocene, volcanic activity began to decline, as evidenced by the presence of carbonate deposits overlying the Southern Mountains Arc. This reduction in volcanic activity during the Middle Miocene across Java is attributed to the progressive advancement of subduction processes. In the Late Miocene, modern volcanic edifices began to develop in eastern West Java, such as Mount Ciremai, which formed atop deformed Upper Miocene volcaniclastic sedimentary deposits.

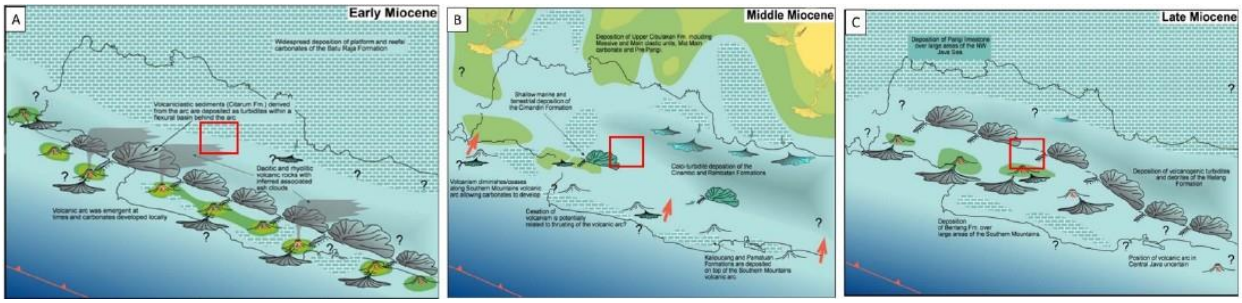

Figure 1. Tectonic evolution of West Java during early to late Miocene (Clements and Hall, 2007).

In greater detail, Abdurrokhim (2017) described the formation of the Jatiluhur Formation within the Bogor Basin using a sequence stratigraphic framework. During the Middle Miocene, the Jatiluhur Formation was deposited under the influence of sea-level fluctuations. This formation exhibits a shallowing-upward pattern within a succession of slope and shelf-margin deposits, consisting predominantly of siliciclastics overlain by limestone.

The geological structures in West Java are generally influenced by the subduction of the Indo-Australian Plate beneath the Eurasian Plate (Hamilton, 1979). The distribution and composition of volcanic centers from the Late Cenozoic to the present demonstrate a clear relationship with the current plate boundary located to the south of Java (Katili, 1975). Java Island displays three principal structural trends: the Meratus trend (southwest–northeast), the Sumatra trend (northwest–southeast), and the Sunda trend (north–south) (Pulunggono and Martodjojo, 1994).

The first trend, the Meratus trend, oriented southwest–northeast, is represented by structures such as the Cimandiri Fault, the Rajamandala Thrust, and other faults in the Purwakarta area. This trend is interpreted as following the arc-shaped pattern of Cretaceous-age structures that extend into the Meratus Mountains in Kalimantan. The second trend, the Sumatra trend, oriented northwest–southeast, is exemplified by the Baribis Fault and faults in the Cimandiri Valley and Gunung Walat region. This structural alignment parallels the trend of the Bukit Barisan Mountains in Sumatra. The third trend, the Sunda trend, is oriented north–south and is represented by the Ciletuh–Seribu Islands alignment (e.g., the Cidurian Fault in the Leuwiliang Block) (Martodjojo, 2003).

According to Hilmi and Haryanto (2008), regional structural patterns in West Java consist of four main fault orientations (Figure 2): northwest–southeast faults, marked by the Citanduy Fault; north–south faults, found in the Bogor–Sukabumi region and extending to Rangkasbitung and Lebak; northeast–southwest faults, represented by the Cimandiri Fault; and east–west faults, typified by the Baribis Fault.

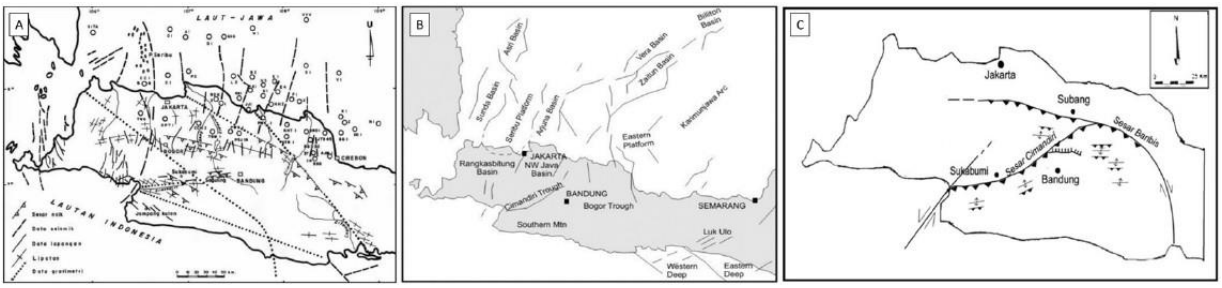

Figure 2. A) General structural trend of West Java (Martodjojo, 2003), B) Regional structural pattern of West and Central Java (Hilmi and Haryanto, 2008), C) Baribis and Cimandiri Fault as regional fault in West Java (Haryanto, 2004; in Hilmi and Haryanto, 2008).

Stratigraphically, the Bogor Basin is divided into three sub-basins: Sanggabuana, Rajamandala, and Sukabumi. According to Abdurrokhim (2017), the study area is located within the Sanggabuana sub-basin of the Bogor Basin, which is composed of the Jatiluhur Formation, Cantayan Formation, Subang Formation, volcanic products, and alluvium (Figure 3). Abdurrokhim (2017) described the sedimentary formations, volcanic deposits, and

alluvial sediments in this basin using a sequence stratigraphic approach. Based on Sudjatmiko (1972), the period of intrusive activity occurred during the Late Miocene, following the deposition of the Cantayan Formation.

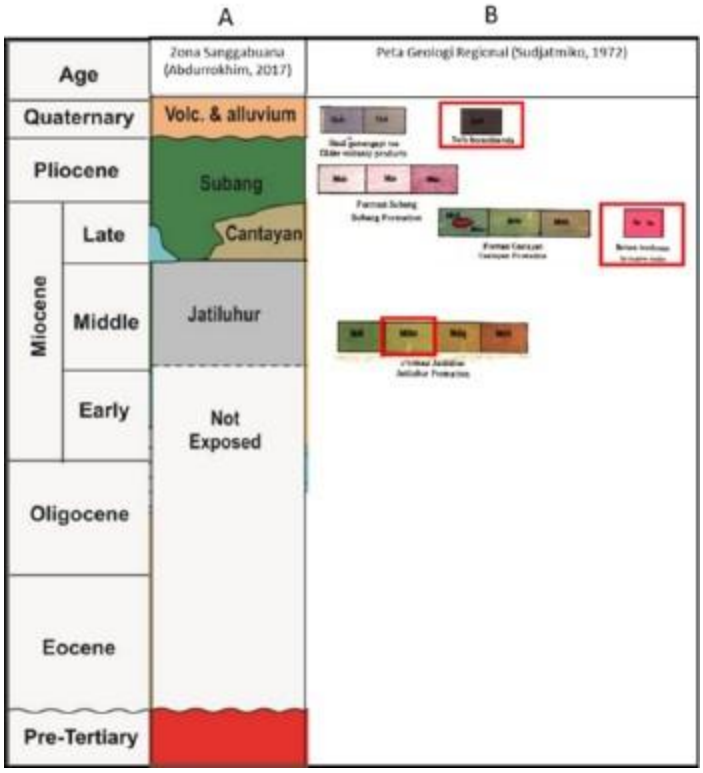

Figure 3. Regional stratigraphy of Bogor Trough, A) Stratigraphy by Abdurrokhim, B) Stratigraphy by Sudjatmiko (based on Abdurrokhim, 2017; Sudjatmiko, 1972).

1. Jatiluhur Formation: Composed predominantly of marl, claystone, and sandstone, with intercalations of limestone.
2. Cantayan Formation: Consists of breccia interbedded with tuffaceous sandstone and shally calcareous claystone.
3. Subang Formation: Composed of breccia, claystone, and sandstone.
4. Old Volcanic and Older Alluvial Deposits: The old volcanic deposits comprise tuffaceous sandstone, cross-bedded tuffaceous clay, and laharic breccia. The older alluvial deposits consist of conglomerate and fluvial sand.
5. Intrusive Rocks: Composed of andesite with mineral assemblages including plagioclase and hornblende.

3. Data and Method

3.1. Data

The data used in this study are thin sections of igneous rocks collected from Mount Parang and Mount Bongkok, which are approximately 1 km apart. A total of 16 rock samples were obtained, consisting of 6 samples from Mount Parang and 10 samples from Mount Bongkok. The spatial distribution of sample acquisition is shown in Figure 4.

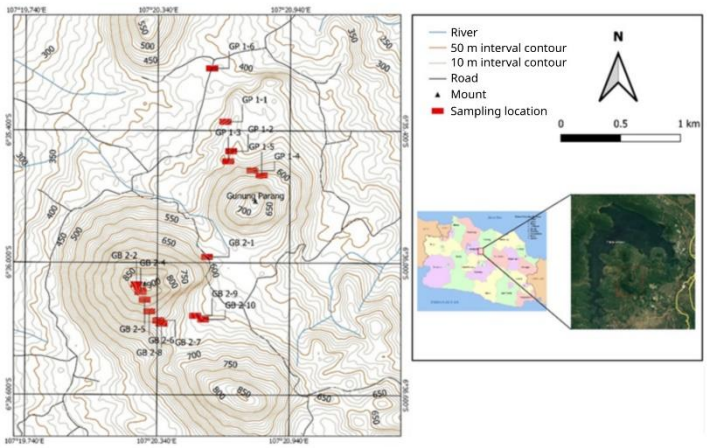

Figure 4. Sampling location map.

3.2. Method

Each prepared thin section was described in terms of its structure, texture, and mineral composition using a BX51 transmitted light polarizing microscope. Digital images were then captured using a digital camera with a 4× objective lens, with each image covering a field of view of approximately 2 mm.

For each acquired image, plagioclase crystals were digitized following the workflow below:

1. Crystals were manually digitized using the ImageJ software (Schneider et al., 2012).
2. The digitized crystals were analyzed to extract shape parameters, including width, length, area, perimeter, centroid location, and orientation.
3. The measured crystal lengths and widths were converted into estimated three-dimensional crystal sizes using the CSDSlice 5 spreadsheet (Morgan and Jerram, 2006).
4. The corrected crystal lengths were then used to classify crystals into phenocrysts (>0.5 mm), microphenocrysts (≥0.1–0.5 mm), and groundmass crystals (<0.1 mm).
5. The shape parameters and aspect ratios obtained from the size conversion were input into the CSDCorrection 1.55 software to calculate population densities and generate CSD (Crystal Size Distribution) plots.
6. The residence time of plagioclase crystals, representing the duration of crystallization, was calculated using the equation from Marsh (1988) (1), where Tc is the crystallization duration in seconds, G is the assumed crystal growth of 10^{-9} mm/s. This value is median range of growth rate given by Cashman (1993). While, m is the slope of the trendline derived from the CSD plot. The conversion factor from seconds to years is 1/31,536,000.

$$Tc = \left(-\frac{1}{G \cdot m}\right) \quad (1)$$

The results from petrographic observations, CSD plots, and crystallization time calculations were integrated to interpret magma dynamics. However, it should be noted that uncertainties might appear from several aspects in CSD, namely non-constant growth-rate relative to crystallization stage (Marsh, 1988), compositional non-selective crystal measurements (Cashman, 2020), and limitation of petrographic observation for groundmass-sized crystals.

4. Result and Discussion

4.1. Petrological Characteristics

4.1.1. Mount Parang

In general, the rocks at Mount Parang are porphyritic andesite, characterized by phenocrysts of plagioclase, pyroxene, and hornblende. In several locations, fragments of basaltic igneous rocks are found embedded within the andesitic host rock (Figure 5). Some plagioclase crystals exhibit sieve texture and zoning (Figure 6). The pyroxene assemblage consists of orthopyroxene and clinopyroxene, with some clinopyroxenes displaying color variations from white to green under plane-polarized light (Table 1). Hornblende appears as prismatic crystals (Figure 6).

Figure 5. (A) Andesite outcrops of Mount Parang observed at outcrops GP 1–6; (B) Hand specimen showing the presence of plagioclase, pyroxene, and hornblende phenocrysts; (C) Basaltic igneous rock fragments enclosed within the andesite.

4.1.2. Mount Bongkok

In general, the rocks at Mount Bongkok are porphyritic andesite, characterized by phenocrysts of plagioclase, pyroxene, and hornblende (Figure 7). In several locations, fragments of basaltic igneous rocks are found embedded within the andesitic body. Some plagioclase crystals exhibit sieve texture and zoning (Figure 8). The pyroxene is composed of prismatic clinopyroxene. Hornblende is also prismatic in habit, with some crystals displaying opaque rims (Figure 8).

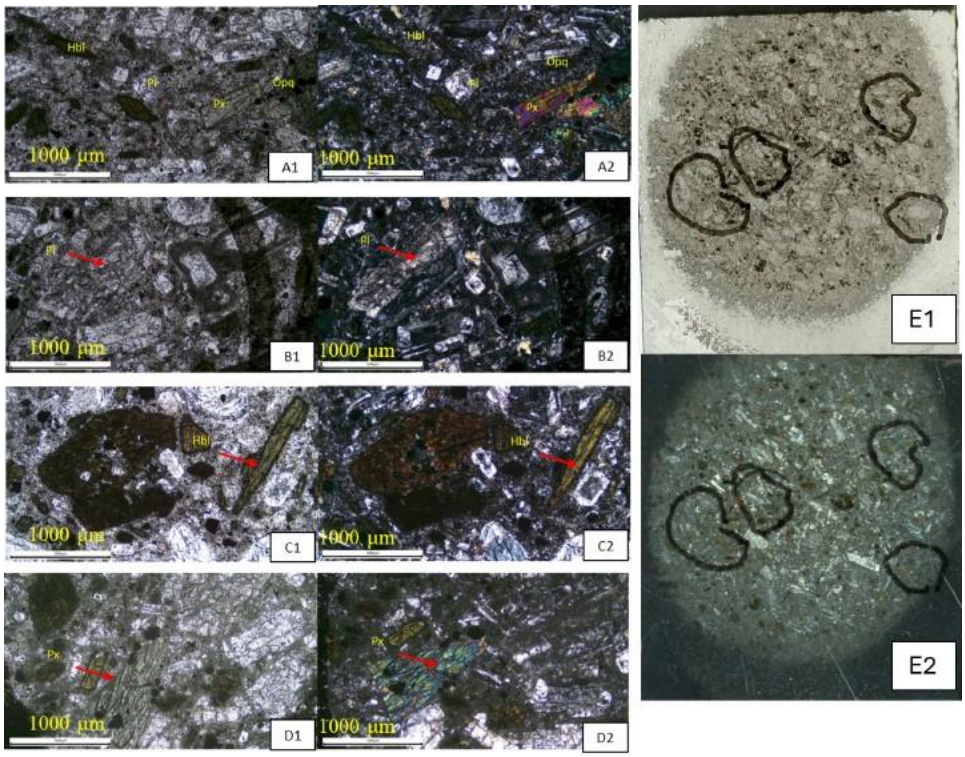

Figure 6. Thin sections of samples GP 1–6, with image index 1 taken under plane-polarized light and index 2 under cross-polarized light; (A) presence of plagioclase and pyroxene phenocrysts; (B) plagioclase exhibiting sieve texture and zoning; (C) hornblende phenocrysts showing opaque rims; (D) pyroxene phenocrysts; (E) full thin-section scan.

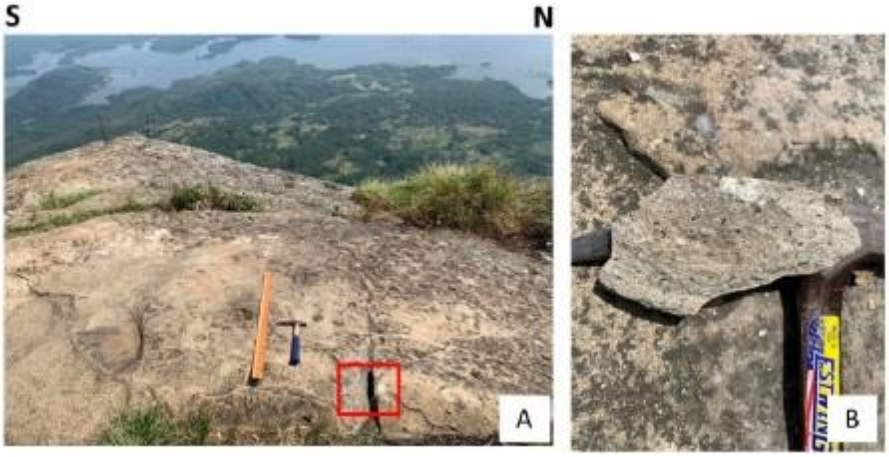

Figure 7. (A) Andesite outcrop of Mount Bongkok at outcrop GB 2–2; (B) Hand specimen showing the presence of plagioclase, pyroxene, and hornblende phenocrysts.

4.2. Crystal Size Distribution

Based on the CSD analysis of the plagioclase histograms (Figure 9), it was observed that the abundance of plagioclase phenocrysts increases toward the central part of the intrusion, while their abundance decreases toward the distal areas. In contrast, the number of microphenocrysts tends to decrease toward the center and increase toward the distal zones. The CSD regression plots further reveal that the gradient becomes gentler toward the central area, whereas it becomes steeper toward the distal margins (Figure 10).

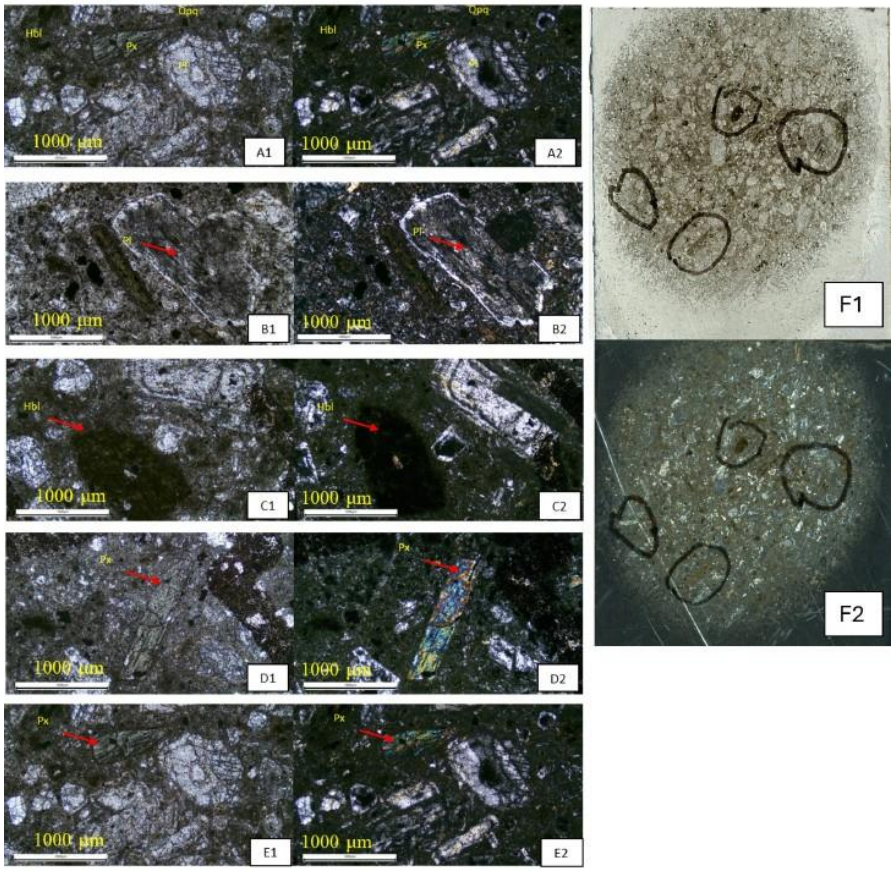

Figure 8. Thin section of sample GB 2–2, with image index 1 taken under plane-polarized light and index 2 under cross-polarized light; (A) presence of plagioclase, hornblende, and pyroxene phenocrysts; (B) plagioclase showing patchy zoning; (C) plagioclase with sieve texture and zoning; (D) and (E) pyroxene phenocrysts; (F) full thin-section scan.

Table 1. Mineralogical composition of andesite samples from Mount Parang and Mount Bongkok.

	Code	Plagioclase	Pyroxene				Hornblende
			Cpx		Opx		
			Colorless	Green	Colorless	Green	
Mt Bongkok	GB 2-2	v	v	v			v
	GB 2-3	v	v	v			v
	GB 2-4	v	v	v		v	v
	GB 2-5	v	v	v		v	v
	GB 2-6	v	v	v			v
	GB 2-7	v	v	v		v	v
	GB 2-8	v	v	v		v	v
	GB 2-9	v	v	v		v	v
	GB 2-10	v	v	v		v	v
	GB 2-1	v	v	v		v	v
Mt Parang	GP 1-4	v					v
	GP 1-3	v		v			v
	GP 1-2	v		v			v
	GP 1-1	v					v
	GP 1-6	v		v			v

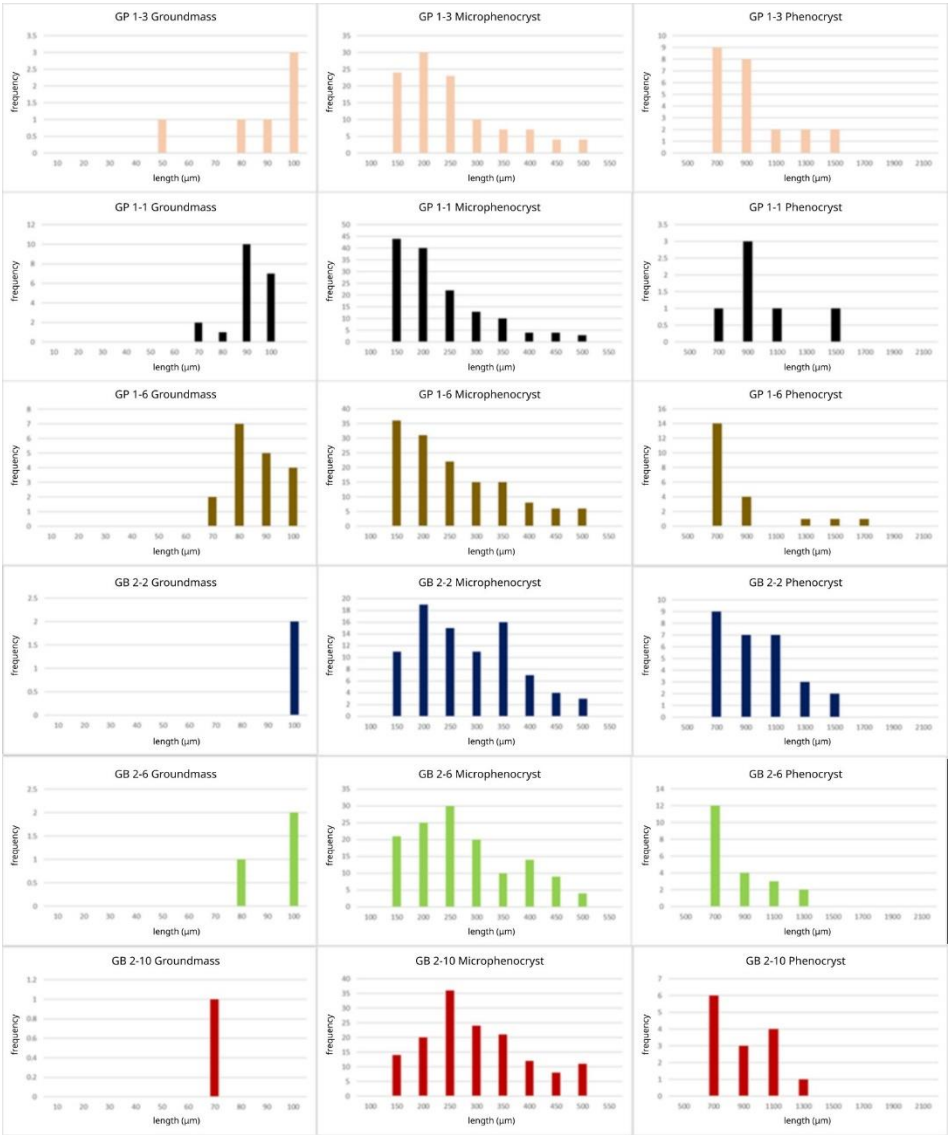

Figure 9. Histogram of plagioclase crystal sizes from Mount Parang (GP) and Mount Bongkok (GB).

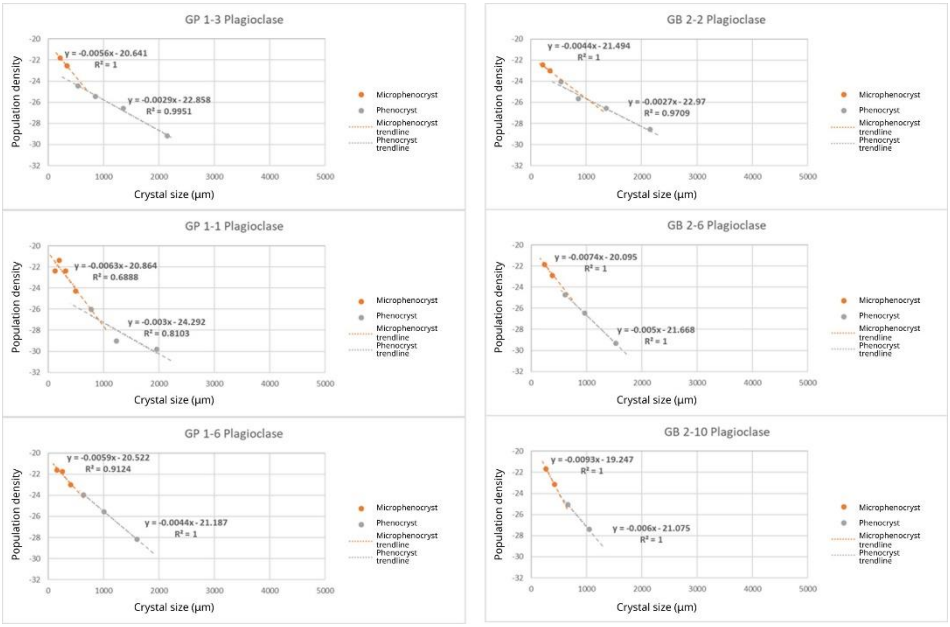

Figure 10. Crystal Size Distribution (CSD) plots of plagioclase from Mount Parang (GP) and Mount Bongkok (GB), showing an increasing gradient from central (top) to distal (bottom) sample positions.

Based on the CSD plots shown in Figure 10, crystallization durations were calculated and are presented in Figure 11. The results indicate that crystallization of plagioclase occurs more rapidly toward the distal parts of the intrusion. The relationship between crystallization time and intrusion geometry is visualized in a graph, where the x-axis represents the sample locations arranged from central (left) to distal (right), and the y-axis represents the calculated crystallization durations (Figure 11).

In the distal zones, plagioclase phenocrysts exhibit crystallization durations ranging from 5 to 7 years, while microphenocrysts range from 3 to 5 years. In the medial section, phenocrysts show crystallization durations of 6 to 10 years, and microphenocrysts range from 4 to 6 years. In the central part, crystallization durations for plagioclase phenocrysts range from 7 to 12 years, while microphenocrysts range from 4 to 7 years.

Cells highlighted in yellow in the table indicate results with high error margins. These elevated errors may be attributed to several factors, including misidentification of minerals, inaccuracies in probability values during mineral identification, or errors in converting mineral dimensions, all of which may lead to incorrect crystallization time estimations.

Code	Gradien (m)		Crystalization Time			
	mm-1		Minutes		Years	
	F	MF	F	MF	F	MF
GB 2-1	-1.80	-2.80	9259259.26	5952380.95	17.62	11.32
GB 2-2	-2.70	-4.40	6172839.51	3787878.79	11.74	7.21
GB 2-3	-3.00	-8.10	5555555.56	2057613.17	10.57	3.91
GB 2-4	-2.80	-7.20	5952380.95	2314814.81	11.32	4.40
GB 2-5	-3.90	-7.60	4273504.27	2192982.46	8.13	4.17
GB 2-6	-5.00	-7.40	3333333.33	2252252.25	6.34	4.29
GB 2-7	-4.00	-1.10	4166666.67	15151515.15	7.93	28.83
GB 2-8	-5.30	-6.00	3144654.09	2777777.78	5.98	5.28
GB 2-9	-4.20	-9.30	3968253.97	1792114.70	7.55	3.41
GB 2-10	-6.00	-9.30	2777777.78	1792114.70	5.28	3.41
GP 1-1	-3.00	-6.30	5555555.56	2645502.65	10.57	5.03
GP 1-2	-2.30	-3.60	7246376.81	4629629.63	13.79	8.81
GP 1-3	-2.90	-5.60	5747126.44	2976190.48	10.93	5.66
GP 1-4	-5.30	-6.60	3144654.09	2525252.53	5.98	4.80
GP 1-6	-4.40	-5.90	3787878.79	2824858.76	7.21	5.37

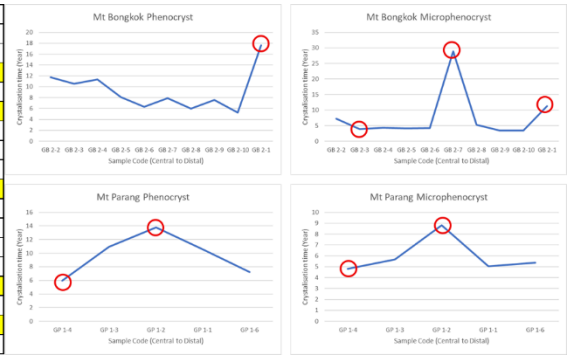

Figure 11. Estimated crystallization durations of plagioclase based on CSD data, and a graph showing the relationship between crystallization time and positions within the intrusive bodies of Mount Parang and Mount Bongkok, including values containing error (shaded yellow and in red circles).

4.3. Cooling Dynamics

4.3.1. Mount Parang

Based on macroscopic observations, petrographic analysis, and CSD analysis of rock samples from Mount Parang, it is interpreted that the magmatic processes involved include magma mixing and assimilation. Evidence of magma mixing is indicated by the presence of zoning and sieve textures in plagioclase crystals.

Furthermore, the gradient trends observed in the CSD plots (Figure 10) also support the interpretation that Mount Parang underwent magma mixing. Signs of magma assimilation are indicated by the presence of basaltoid rock fragments observed macroscopically at several outcrops near the margins (GP 1–6). Pyroxene crystals in Mount Parang exhibit signs of oxidation, as evidenced by the presence of rims surrounding the pyroxene. Oxidation in pyroxene occurs while the magma is still in a molten state. This process was facilitated by the release of water under subsurface pressure and temperature conditions, which increases the oxygen content in the magma. The influence of the oxygen gradient during crystallization is associated with gas release, which promotes cation mobility to overcome the activation energy required for diffusion, nucleation, and crystal growth (Burkhard, 2001). Gas release in Mount Parang is further supported by the occurrence of patchy zoning which was formed under conditions of fluctuating pressure and temperature. It caused water to exsolve from the melt, thereby increasing the oxygen fugacity within the magma (Humphreys et al., 2006).

Crystallization duration calculations for plagioclase (Figure 11) show that samples from GP 1–6 exhibit the shortest crystallization times, with phenocrysts crystallizing over approximately 7.21 years and microphenocrysts over 5.37 years. In contrast, samples from the deeper zone (GP 1–3) record longer crystallization times of approximately 10.93 years (~11 years) for phenocrysts and 5.66 years (~6 years) for microphenocrysts. Macroscopically, crystals in samples from GP 1–6 are finer-grained, which supports the interpretation that these rocks crystallized earlier due to their proximity to the intrusion margins. The crystallization time data for plagioclase further confirm that crystallization occurred more rapidly toward the distal parts of the intrusion (Figure 12).

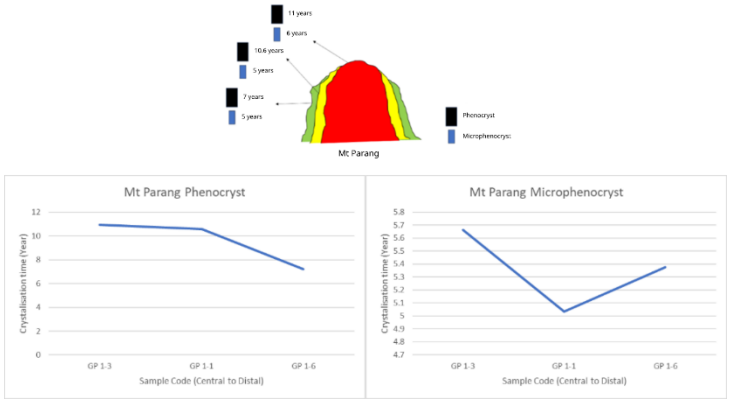

Figure 12. Schematic illustration of cooling at Mount Parang, showing a general trend of decreasing crystallization duration from central to distal.

4.3.1. Mount Bongkok

Based on macroscopic observations, petrographic analysis, and CSD analysis of rock samples from Mount Bongkok, it is interpreted that the magmatic processes involved include magma mixing and assimilation. Evidence of magma mixing is indicated by the presence of zoning and sieve textures in plagioclase observed under the microscope. Furthermore, the gradient trends from the CSD plots (Figure 10) show patterns consistent with magma mixing in samples from Mount Bongkok.

Assimilation is inferred from the presence of rock fragments found at several marginal outcrops (GB 2-1, GB 2-8, GB 2-9, and GB 2-10). Oscillatory zoning observed in plagioclase crystals at Mount Bongkok indicates that crystallization occurred under conditions of high partial pressure of H_2O, followed by resorption during decompression when H_2O became undersaturated (Humphreys et al., 2006).

Crystallization time calculations for plagioclase (Figure 11) reveal that GB 2-10 exhibits the shortest crystallization durations, with approximately 5.28 years for phenocrysts and 3.41 years for microphenocrysts. In contrast, the deepest sample, GB 2-2, shows crystallization durations of approximately 11.74 years (~12 years) for phenocrysts and 7.21 years (~7 years) for microphenocrysts. Macroscopically, crystals in GB 2-10 are fine-grained, supporting the interpretation that crystallization occurred earlier due to its location near the intrusion margin. The crystallization time data from Mount Bongkok indicates that crystallization proceeded more rapidly toward the distal parts of the intrusion (Figure 13), consistent with the observed decrease in crystal size toward the margins.

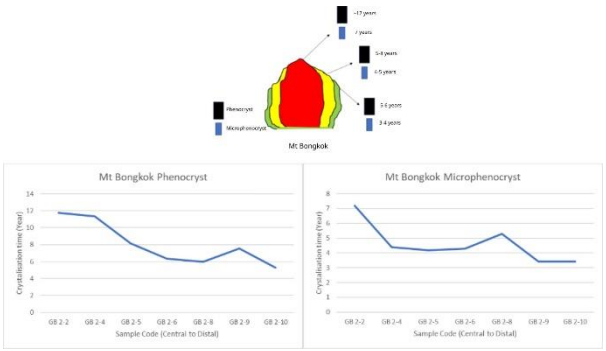

Figure 13. Schematic illustration of cooling at Mount Bongkok, showing a general trend of decreasing crystallization duration from interior to exterior.

4.4. Formation of Mount Parang dan Mount Bongkok

The reconstruction of the formation of Mount Parang and Mount Bongkok, based on literature, field observations, petrographic analysis, and CSD data, can be arranged within a crystallization timeframe (Figure 14). Three key time points can be identified: the initial stage when both bodies were still dominantly molten magma (T0), the point of complete solidification (T4; Late Miocene according to Sudjatmiko, 1972), and the time of exposure at the surface (T5). Between T0 and T4, additional time points can be determined based on the CSD calculations. The duration framework used to define these time points includes:

ΔF = duration of phenocryst crystallization.
ΔmF = duration of microphenocryst crystallization.
Δmd = duration of groundmass crystallization (not calculated in this study).

At T0, both mountains were predominantly molten magma. The presence of orthopyroxene at Mt Bongkok indicates a slight difference in bulk compositional content compared to Mt. Parang. In addition, initial crystallization temperatures might also differ for both mountains. It may imply two possibilities: they came from different melts (spatially or temporally), or they came from the same melt but quickly differentiated during ascend. Detailed geochemical analysis need to be conducted to resolve this issue.

At T1, phenocryst crystallization began with nucleation followed by crystal growth, occurring as the magma ascended. During phenocryst growth, a magma injection event disrupted the crystal-melt equilibrium, recorded in plagioclase as sieve textures. Once a new equilibrium was established, plagioclase resumed growth, forming zones around the sieve zones, leading to the complete development of phenocrysts by T2. This entire process from T0 to T2 occurred over the period ΔF.

In between T1 and T2, different processes happened at Mt. Parang and Mt. Bongkok. Magma of Mt. Parang underwent increase of oxygen content and degassing which produced oxide rims on pyroxene and patchy zoning in plagioclase (Burkhard, 2001; Humphreys et al., 2006). In contrast, gas release at Mt. Bongkok resulted only in formation of oscillatory zoning (Humphreys et al., 2006).

Subsequently, microphenocrysts nucleated and grew until T3 over the duration ΔmF. In the final phase, the groundmass crystallized over Δmd, until complete solidification was achieved in the Late Miocene (T4). Between T0 and T4, the incorporation of country rock into the magma body likely occurred, recorded as basaltoid fragments. Following full crystallization, uplift and erosion exposed the intrusive bodies, now recognized as Mount Parang and Mount Bongkok (T5).

Thus, the total time required for complete crystallization from the molten phase is estimated as ΔF + ΔmF of the central crystal population, which are 16.59 years for Mount Parang and 18.95 years for Mount Bongkok before counting for groundmass cooling duration (Δmd). However, this assumes sequential crystallization of each crystal size group, whereas in natural systems, smaller crystals may begin crystallizing before larger crystals have finished growing. If phenocrysts and microphenocrysts are assumed to cease growing simultaneously, the crystallization duration of both mountains may be better represented by ΔF, amounting to 11.74 years for Mount Parang and 10.93 years for Mount Bongkok before counting for groundmass cooling duration (Δmd).

In terms of cooling duration, a more thorough calculation, especially for intrusive body should account for cooling duration of the groundmass (Δmd). It means that longer cooling duration will

be produced. It should be noted as well that possible change in crystallization rate during different stage of cooling (Marsh, 1988) might affect the calculation of total cooling time. In addition, difference in cooling depth may also contribute to change in cooling rate (Garrido et al., 2001) which can render generalization in phenocryst cooling time irrelevant. For this reason, more thorough composition-based analysis on phenocryst that may infer termo-barometric condition will be needed for the calculation (e.g. Higgins, 2017; Martin et al., 2010).

Overall, the magma dynamics and crystallization timescales observed in the formation of Mt. Parang and Mt. Bongkok may be representative of processes occurring in other sub-volcanic intrusive complexes of similar age in West Java. However, future studies that reference these findings should account for potential variations arising from differences in bulk magma composition and the nature of surrounding wall rocks.

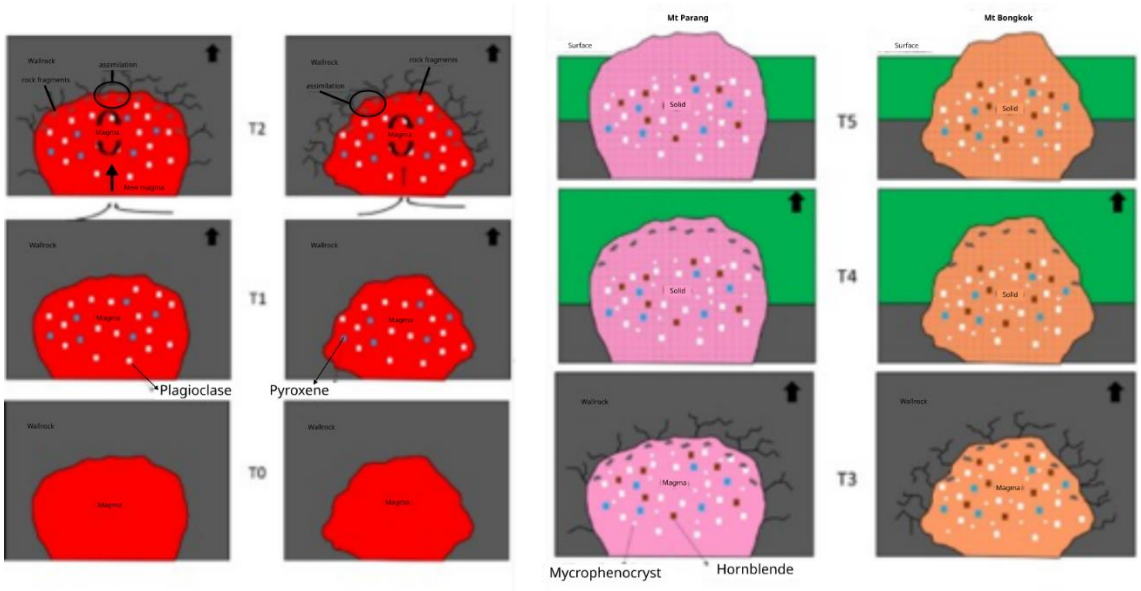

Figure 14. Schematic reconstruction of the formation of Mount Parang and Mount Bongkok at successive time intervals, based on the crystallization timeframe of plagioclase crystal populations.

5. Conclusion

Based on the observations and calculations conducted, the following conclusions were drawn:

- Mount Parang and Mount Bongkok are composed of andesite containing phenocrysts of plagioclase, pyroxene, and amphibole with slight bulk compositional differences.
- Evidence of magma mixing and assimilation was identified during the crystallization processes in both intrusions.
- The estimated crystallization duration for Mount Parang is around 11.74–16.59 years before counting for the crystallization of the groundmass.
- The estimated crystallization duration for Mount Bongkok is around 10.93–18.95 years before counting for the crystallization of the groundmass.
- The processes and timing of Mt. Parang and Mt. Bongkok might be analogous to other intrusive complexes of similar age in West Java.

Acknowledgements

The authors would like to thank the anonymous reviewer for the valuable feedback provided, which greatly contributed to the final form of this manuscript.

Author Contributions

BP conducted data acquisition, petrographic observation, CSD acquisition and processing, and manuscript writing. RPN conceived the research idea, carried out petrographic observation, and contributed to manuscript writing.

6. References

Abdurrokhim, A., 2017. Stratigrafi Sikuen Formasi Jatiluhur di Cekungan Bogor Jawa Barat. Bulletin of Scientific Contribution: GEOLOGY 15, 167–172.

Arfiansyah, K., Helmi, F., 2018. Genesis amfibol pada diorit Pasir Cupu, Kecamatan Plered, Kabupaten Purwakarta, Jawa Barat.

Bulletin of Scientific Contribution: GEOLOGY 16, 183–194.
Ashok, Ch., Santhosh, G.H.N.V., Ratnakar, J., Dash, S., 2022. Magma Mixing and Mingling during Pluton Formation: A Case Study through Field, Petrography and Crystal Size Distribution (CSD) Studies on Sirsilla Granite Pluton, India. Journal of the Geological Society of India 98, 815–821. https://doi.org/10.1007/s12594-022-2072-4
Burkhard, D.J., 2001. Crystallization and oxidation of Kilauea basalt glass: processes during reheating experiments. Journal of Petrology 42, 507–527.
Cashman, K.V., 2020. Crystal Size Distribution (CSD) Analysis of Volcanic Samples: Advances and Challenges. Front. Earth Sci. 8, 291. https://doi.org/10.3389/feart.2020.00291
Cashman, K.V., 1993. Relationship between plagioclase crystallization and cooling rate in basaltic melts. Contributions to Mineralogy and Petrology 113, 126–142.
Clements, B., Hall, R., 2007. Cretaceous to Late Miocene stratigraphic and tectonic evolution of West Java, in: Proc. Indon Petrol. Assoc., 31st Ann. Conv. Presented at the Thirty-First Annual Convention, Indonesian Petroleum Association (IPA). https://doi.org/10.29118/IPA.1520.07.G.037
Garrido, C.J., Kelemen, P.B., Hirth, G., 2001. Variation of cooling rate with depth in lower crust formed at an oceanic spreading ridge: Plagioclase crystal size distributions in gabbros from the Oman ophiolite. Geochem Geophys Geosyst 2. https://doi.org/10.1029/2000gc000136
Hamilton, W.B., 1979. Tectonics of the Indonesian region. US Govt. Print. Off.
Haryanto, I., 2004. Tektonik Sesar Baribis-Cimandiri. Prosiding tahunan IAGI 33.
Higgins, M.D., 2017. Quantitative investigation of felsic rock textures using cathodoluminescence images and other techniques. Lithos 277, 259–268. https://doi.org/10.1016/j.lithos.2016.05.006
Hilmi, F., Haryanto, I., 2008. Pola Struktur Regional Jawa Barat. Bulletin of Scientific Contribution 6, 57–66.
Humphreys, M.C.S., Blundy, J.D., Sparks, R.S.J., 2006. Magma Evolution and Open-System Processes at Shiveluch Volcano: Insights from Phenocryst Zoning. Journal of Petrology 47, 2303–2334. https://doi.org/10.1093/petrology/egl045
Katili, J.A., 1975. Volcanism and plate tectonics in the Indonesian island arcs. Tectonophysics 26, 165–188.
Lestianingrum, D., Wijaya, B., 2020. Pembagian zona alterasi Daerah Tajursindang dan sekitarnya Provinsi Jawa Barat. Journal of Geoscience Engineering and Energy 1, 153–162.
Magee, C., O'driscoll, B., Chambers, A.D., 2010. Crystallization and textural evolution of a closed-system magma chamber: insights from a crystal size distribution study of the Lilloise layered intrusion, East Greenland. Geological Magazine 147, 363–379. https://doi.org/10.1017/S0016756809990689
Marsh, B.D., 1988. Crystal size distribution (CSD) in rocks and the kinetics and dynamics of crystallization: I. Theory. Contributions to Mineralogy and Petrology 99, 401–415. https://doi.org/10.1007/BF00371933
Martin, V.M., Davidson, J., Morgan, D., Jerram, D.A., 2010. Using the Sr isotope compositions of feldspars and glass to distinguish magma system components and dynamics. Geology 38, 539–542. https://doi.org/10.1130/G30758.1
Martodjojo, S., 2003. Evolusi Cekungan Bogor Jawa Barat. Penerbit ITB Bandung 239.
Morgan, D.J., Jerram, D.A., 2006. On estimating crystal shape for crystal size distribution analysis. Journal of Volcanology and Geothermal Research 154, 1–7. https://doi.org/10.1016/j.jvolgeores.2005.09.016
Patwardhan, K., Marsh, B.D., 2011. Dynamics of the Development of the Isle au Haut Gabbro–Diorite Layered Complex: Quantitative Implications for Mafic–Silicic Magma Interactions. Journal of Petrology 52, 2365–2395. https://doi.org/10.1093/petrology/egr049
Pulunggono, A. d, Martodjojo, S., 1994. Perubahan tektonik Paleogen-Neogen merupakan peristiwa tektonik terpenting di Jawa. Proc. Geologi dan Geoteknik Pulau Jawa, Yogyakarta, h 37–49.
Schneider, C.A., Rasband, W.S., Eliceiri, K.W., 2012. NIH Image to ImageJ: 25 years of image analysis. Nature Methods 9, 671–675. https://doi.org/10.1038/nmeth.2089
Sobolev, S.N., Ariskin, A.A., Nikolaev, G.S., Pshenitsyn, I.V., 2023. Crystal Size Distribution as a Key to Understanding Protocumulus Evolution in Layered Intrusions: Experiments, Calculations, and Practice of CSD Extraction. Petrology 31, 648–663. https://doi.org/10.1134/S0869591123060097
Sudjatmiko, S., 1972. Peta Geologi Lembar Cianjur, Jawa Barat.